Chemical Approach to the Cu(II)-Phenoxyl Radical Site in Galactose Oxidase: Dependence of the Radical Stability on N-Donor Properties

Yuichi Shimazaki, Stefan Huth, Shun Hirota, and Osamu Yamauchi*

Department of Chemistry, Graduate School of Science and Research Center for Materials Science, Nagoya University, Nagoya 464-8602

(Received December 10, 1999)

Copper(II) complexes of several new N_3O-type tripodal ligands, 2,4-di(*t*-butyl)-6-{[bis(2-pyridyl)methyl]aminomethyl}phenol (HtbuL), 2,4-di(*t*-butyl)-6-{[(6-methyl-2-pyridyl)methyl](2-pyridylmethyl)aminomethyl}phenol (HtbuL(Mepy)), 2,4-di(*t*-butyl)-6-{bis[(6-methyl-2-pyridyl)methyl]aminomethyl}phenol (HtbuL$(Mepy)_2$), and 2,4-di(*t*-butyl)-6-{[(1-methyl-2-imidazolyl)methyl][(6-methyl-2-pyridyl)methyl]aminomethyl}phenol (HtbuL(im)(Mepy)), were prepared. They were structurally characterized by the X-ray crystallographic method to have a square-pyramidal structure with a weakly coordinating group at an apical position. The phenol moiety of [CuCl(tbuL(Mepy))] (**2**), [CuCl(tbuL$(Mepy)_2$)] (**3**), and [CuCl(tbuL(im)(Mepy))] (**4**) was revealed to be coordinated equatorially; it was converted to the phenoxyl radical upon oxidation with Ce(IV), giving a new absorption peak at 405—420 nm. ESR measurements at low temperatures and resonance Raman spectra established that the radical species has a Cu(II)-phenoxyl radical bond. The cyclic voltammograms exhibited a quasi-reversible redox wave at $E_{1/2}$ = 0.56—0.61 V (vs. Ag/AgCl) corresponding to the formation of the phenoxyl radical, which displayed a first order decay with a half life of 65 and 62 min at −20 °C for **2** and **4**, respectively, while that for **3** was only 9.0 min at −40 °C. The radical stability increased with the donor ability of the equatorial N ligands.

Galactose oxidase (GO)[1] is a single-copper oxidase, which catalyzes the conversion of primary alcohols to aldehydes in the presence of dioxygen. X-ray structural analysis has disclosed that the copper site has a square-pyramidal structure with two imidazole nitrogens and one phenoxide oxygen in the equatorial positions and an axial phenol moiety interacting only weakly with the copper ion (Fig. 1).[2] The equatorial phenolate ring is covalently linked to a cysteine residue via a carbon-sulfur bond. GO performs the two-electron oxidation with the aid of this phenoxo ligand, which functions as a cofactor by forming a phenoxyl radical in the catalytic cycle.[1—4]

The active form of GO has a Cu(II)-phenoxyl radical bond,

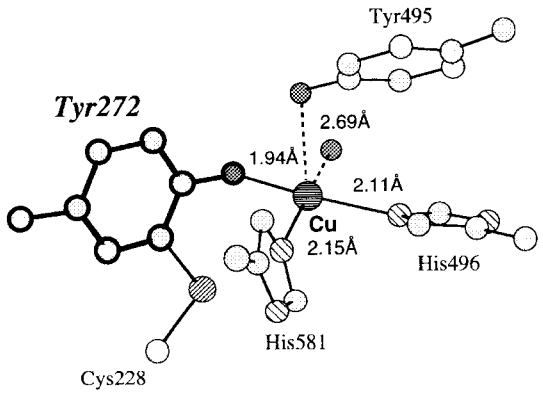

Fig. 1. Structure of the active site of GO.[2]

which is EPR inactive due to the antiferromagnetic interaction between the two $S = 1/2$ centers.[5] The X-ray absorption edge structures indicated the presence of the Cu(II) ion,[6] and the diagnostic phenoxyl radical vibration has been assigned in the resonance Raman spectra.[7] GO exhibits an intense optical absorption maximum at 444 nm (ε = 5194) due in part to a π–π^* transition of the Cu(II)-coordinated phenoxyl radical, which is more stable than the free phenoxyl radical.[1,3,4] The redox potential for the formation of the Cu(II)-phenoxyl radical species in GO is 0.41V, which is considerably lower than that for the free phenoxyl radical (0.94 V).[8] Upon oxidation of a primary alcohol to the aldehyde, the radical species is reduced to the Cu(I)-phenol state by a two-electron process. The oxidized species is subsequently restored by a two-electron oxidation by dioxygen, which is itself reduced to H_2O_2.[1—4]

A number of studies have been reported on model complexes of the GO active site; Wieghardt et al.[9a,9b] and Tolman et al.[10a,10b] successfully characterized the Cu site by complexes using the 1,4,7-triazacyclononane skeleton with one, two, or three phenol/phenoxide moieties coordinated to the Cu(II) ion; complexes containing a phenoxyl radical site with Cu(II) and other metal ions have also been prepared.[11] The phenoxyl radical-metal ion binding has been further characterized by other groups,[12] and efficient functional models for GO have been studied by Stack et al.,[13] who introduced a binaphthyl group to make the copper coordination structure more rigid and attained catalytic oxidation of primary

alcohols. Very recently, Wieghardt et al. also succeeded in catalytic oxidation of ethanol by functional copper and zinc complexes of a new 1,2-phenylenediamine derivative with two phenol moieties.[9c—9e] By using a new ligand, *N*-(2-pyridylmethyl)bis(3,5-di-*t*-butyl-2-hydroxybenzyl)amine, and copper(II) acetate, we recently prepared a GO structural model that mimics the coordination mode of the Cu site.[14] This Cu(II)-ligand system exhibited reactivities depending on the nature of the counteranion, and with $Cu(ClO_4)_2$ we observed a spontaneous formation of the phenoxyl radical via disproportionation.

In order to obtain further information on the formation and bonding mode of the Cu(II)-radical species, we have now synthesized Cu(II) complexes of ligands with varying equatorial N donors (Fig. 2) and investigated the influence of the ligand donor ability[15] on the copper site structure and formation and stability of the phenoxyl radical species.

Experimental

Materials and Methods. All reagents were used as received except CH_3CN which was dried with CaH_2. Electronic spectra were obtained with a Shimadzu UV-3101PC spectrophotometer. The kinetics of the decay of Cu complexes in CH_3CN under anaerobic conditions were measured spectrophotometrically. Electrochemical measurements were made with a Hokuto Denko HB-104 function generator and an HA-104 potentio/galvanostat or with a BAS 100B electrochemical analyzer. A conventional three-electrode cell was used with a 3-mm diameter glassy-carbon electrode as working electrode, a platinum wire as counter electrode, and a Ag/AgCl electrode as reference electrode. Cyclic voltammograms were recorded for samples (10^{-3} M; M = mol dm^{-3}) dissolved in dry CH_3CN containing 0.1 M tetrabutylammonium perchlorate (TBAP). The reversibility of the electrochemical processes was evaluated by standard procedures and referenced against the ferrocene/ferrocenium redox couple. Frozen solution ESR spectra at 77 K were acquired by a JEOL JES-RE1X X-band spectrometer equipped with standard low-temperature apparatus. ESR spectra at 4—50 K were obtained by a Bruker ESP 300E spectrometer equipped with a helium flow cryostat. All spectra were recorded by using 4-mm inner diameter quartz tubes. Microwave frequency was standardized against the Mn(II) marker. Resonance Raman spectra were excited at 457.9 nm with an Ar^+ laser and detected with a JASCO NR-1800 triple polychromator equipped with a liquid-nitrogen-cooled Princeton Instruments CCD detector. Raman measurements were carried out with a spinning cell and the laser power was adjusted to 50 mW at the sample point. Raman shifts were calibrated with acetone, the accuracy of the peak positions of the Raman bands being ± 1 cm^{-1}.

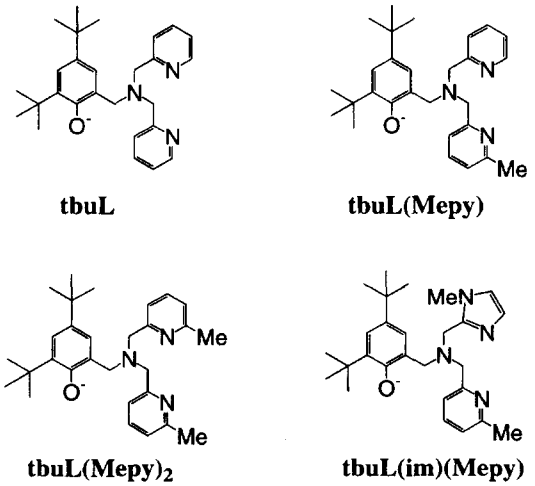

Fig. 2. Structures of ligands.

2,4-Di(*t*-butyl)-6-{[bis(2-pyridyl)methyl]aminomethyl}phenol (HtbuL). To a solution of 3,5-di(*t*-butyl)-2-hydroxybenzaldehyde (2.34 g, 10 mmol) in methanol (100 ml) were added bis(2-pyridylmethyl)amine (1.99 g, 10 mmol) and a small amount of acetic acid. Sodium cyanotrihydroborate (0.63 g, 10 mmol) was added dropwise to the resulting solution with stirring. After the solution was stirred for three days at room temperature, it was acidified by adding concd HCl and then evaporated almost to dryness under a reduced pressure. The residue was dissolved in saturated aqueous Na_2CO_3 (50 ml) and extracted with $CHCl_3$ (3×50 ml). The combined extracts were dried over anhydrous Na_2SO_4 and evaporated almost to dryness under reduced pressure to give a brown oil, which was purified on a silica-gel column with chloroform–methanol. Yield 3.00 g (72.0%). ^{1}H NMR ($CDCl_3$, 300 MHz) δ = 1.26 (s, 9H), 1.45 (s, 9H), 3.80 (s, 2H), 3.87 (s, 4H), 6.88 (d, 1H), 7.15 (m, 2H), 7.20 (d, 1H), 7.37 (d, 2H), 7.63 (t, 2H), 8.55 (d, 2H), 10.6 (br, 1H).

The following ligands were prepared in a similar manner and isolated in 67.5, 70.4, and 64.1% yields, respectively, by silica gel column chromatography.[15]

2,4-Di(*t*-butyl)-6-{[(6-methyl-2-pyridyl)methyl](2-pyridylmethyl)aminomethyl}phenol (HtbuL(Mepy)). ^{1}H NMR ($CDCl_3$, 300 MHz) δ = 1.26 (s, 9H), 1.46 (s, 9H), 2.58 (s, 3H), 3.77 (s, 2H), 3.84 (s, 2H), 3.86 (s, 2H), 6.88 (d, 1H), 7.01 (d, 1H), 7.12 (d, 1H), 7.14 (dd, 1H), 7.20 (d, 1H), 7.41 (d, 1H), 7.51 (t, 1H), 7.61 (dt, 1H), 8.53 (d, 1H), 10.6 (br, 1H).

2,4-Di(*t*-butyl)-6-{bis[(6-methyl-2-pyridyl)methyl]aminomethyl}phenol (HtbuL(Mepy)$_2$). ^{1}H NMR ($CDCl_3$, 300 MHz) δ = 1.26 (s, 9H), 1.46 (s, 9H), 2.58 (s, 6H), 3.75 (s, 2H), 3.83 (s, 4H), 6.88 (d, 1H), 6.99 (d, 2H), 7.17 (d, 2H), 7.19 (d, 1H), 7.51 (t, 2H), 10.6 (br, 1H).

2,4-Di(*t*-butyl)-6-{[(1-methyl-2-imidazolyl)methyl][(6-methyl-2-pyridyl)methyl]aminomethyl}phenol (HtbuL(im)(Mepy)). ^{1}H NMR ($CDCl_3$, 300 MHz) δ = 1.26 (s, 9H), 1.46 (s, 9H), 2.62 (s, 3H), 3.40 (s, 3H), 3.71 (s, 2H), 3.74 (s, 2H), 3.83 (s, 2H), 6.70 (d, 1H), 6.86 (d, 1H), 6.93 (d, 1H), 6.95 (d, 1H), 6.99 (d, 1H), 7.24 (d, 1H), 7.49 (t, 1H), 10.6 (br, 1H).

[CuCl(HtbuL)]ClO_4 (1). To a solution of HtbuL (0.409 g, 1.0 mmol) in methanol (10 ml) was added dropwise a solution of $CuCl_2 \cdot 2H_2O$ (0.085 g, 0.5 mmol) and $Cu(ClO_4) \cdot 6H_2O$ (0.185 g, 0.5 mmol) in methanol (10 ml). After standing for a few hours at room temperature, the reaction mixture gave microcrystals, which were recrystallized from CH_3CN–diethyl ether. Yield 0.414 g (67%). Found: C, 51.97: H, 6.30; N, 6.80%. Calcd for $C_{27}H_{37}Cl_2CuN_3O_5$: C, 52.47; H, 6.03; N, 6.80%.

[CuCl(tbuL(Mepy))] (2). To a solution of HtbuL(Mepy) (0.433 g, 1.0 mmol) in methanol (10ml) was added $CuCl_2 \cdot 2H_2O$ (0.170 g, 1.0 mmol) in methanol (10 ml). Triethylamine (a few drops) was added to the resulting solution, which was kept standing for a few days at room temperature. The microcrystals obtained were recrystallized from CH_3CN–methyl acetate. Yield 0.363 g (68.2%). Found: C, 63.34; H, 6.99; N, 7.87%. Calcd for $C_{28}H_{38}ClCuN_3O$: C, 63.50; H, 6.85; N, 7.93%.

The following complexes were prepared in a similar manner in 65 and 74% yields, respectively.

[CuCl(tbuL(Mepy)$_2$)] (3). Found: C, 63.64; H, 7.35; N, 7.75%. Calcd for $C_{29}H_{40}ClCuN_3O$: C, 63.84; H, 7.39; N, 7.70%.

[CuCl(tbuL(im)(Mepy))] (4). Found: C, 60.50; H, 7.11; N, 10.4%. Calcd for $C_{27}H_{38}ClCuN_4O$: C, 60.77; H, 7.18; N, 10.5%.

[ZnCl(tbuL)]. This complex was prepared as colorless crystals in a similar manner to that for **2** from HtbuL (0.417 g, 1.0 mmol) and $ZnCl_2$ (0.136 g, 1.0 mmol) in CH_3CN. Found: C, 61.10; H, 6.70; N, 7.86%. Calcd for $C_{27}H_{36}ClN_3OZn$: C, 60.57; H, 7.11; N, 7.80%.

X-Ray Structure Determination of Cu(II) Complexes. All the X-ray measurements were carried out on a Rigaku AFC-5R four-circle automated diffractometer with graphite monochromated Cu $K\alpha$ radiation (λ = 1.54178 Å) and a rotating anode generator. The crystals were mounted on a glass capillary. The reflection intensities for **1**, **2**, **3**, and **4** were monitored by three standard reflections for every 2 h or 150 measurements, which indicated that the decays of intensities for all crystals were within 2%. Reflection data were corrected for both Lorentz and polarization effects. The structures were solved by the heavy-atom method and refined anisotropically for non-hydrogen atoms by full-matrix least-squares calculations. Each refinement was continued until all shifts were smaller than one third of the standard deviations of the parameters involved. Atomic scattering factors and anomalous dispersion terms were taken from the literature.[16] Hydrogen atoms for all structures were located at the calculated positions except for the phenol-OH group and were assigned a fixed displacement and constrained to ideal geometry with C–H = 0.95 Å. The thermal parameters of calculated hydrogen atoms were related to those of their parent atoms by $U(H) = 1.2U_{eq}(C)$. The hydrogen atom of the phenol-OH group of **1** was located from the difference Fourier map. All the calculations were performed by the TEXSAN program package.[17] Summaries of the fundamental crystal data and experimental parameters for structure determination are given in Table 1. Tables of positional parameters and B(eq)'s, anisotropic displacement parameters, and observed and calculated structure factors for the complexes are deposited as Document No. 73027 at the Office of the Editor of Bull. Chem. Soc. Jpn. Crystallographic data have been deposited at the CCDC, 12 Union Road, Cambridge CB2 1EZ, UK, and copies can be obtained on request, free of charge, by quoting the publication citation and the deposition numbers 139975-139978.

Results and Discussion

Description of Structures. The ORTEP views of complexes **1**, **2**, **3**, and **4** are shown in Figs. 3, 4, 5, and 6, respectively, and the selected bond lengths and angles are listed in Table 2. All the complexes were mononuclear, with one chloride ion equatorially coordinated to the Cu center.

From the Cu(1)–O(1) distance of 2.567(5) Å in **1**, which is significantly longer than that for the apical phenoxide (2.174(3)—2.268(2) Å) in [Cu(bpnp)X] (X = Cl^-, SCN^-, CH_3COO^-; bpnp = 2-[bis(2-pyridylmethyl)amino]methyl-4-nitrophenol)[18] and for the apical phenol (2.40 Å (average)) in [Cu(HL)CH_3COO] (H_2L = *N*-(2-pyridylmethyl)bis(3,5-di-*t*-butyl-2-hydroxybenzyl)amine),[14] we conclude that this protonated phenol moiety coordinates only weakly to the Cu(II) ion (Fig. 3). The Cu(II) ion coordinates two pyridine nitrogen atoms, one tertiary nitrogen atom, and a chloride ion with the Cu–N bond lengths Cu(1)–N(1) = 1.982(5), Cu(1)–N(2) = 2.043(4), and Cu(1)–N(3) = 1.980(6) Å in a geometry that can be described as distorted square-pyramidal. The relative extent of the trigonal-bipyramidal distortion is indicated by an index τ representing the degree of trigonality within the structural continuum between square-planar and trigonal-bipyramidal structures.[19] The τ value of the Cu

Table 1. Crystallographic Data for [CuCl(HtbuL)]CLO_4 (**1**), [CuCl(tbuL(Mepy))] (**2**), [CuCl(tbuL(Mepy)$_2$)] (**3**), and [CuCl(tbuL(im)(Mepy))] (**4**)

Complex	**1**	**2**	**3**	**4**
Formula	$C_{27}H_{37}Cl_2CuN_3O_5$	$C_{28}H_{38}ClCuN_3O$	$C_{29}H_{40}ClCuN_3O$	$C_{27}H_{38}ClCuN_4O$
Formula weight	618.06	531.63	545.65	533.62
Crystal system	Triclinic	Monoclinic	Monoclinic	Orthorhombic
Space group	$P\bar{1}$	$P2/c$	$P2/c$	$P2_12_12_1$
a/Å	11.948(4)	15.351(5)	15.667(3)	13.056(2)
b/Å	12.028(3)	10.138(5)	10.265(1)	24.906(6)
c/Å	10.830(4)	17.580(5)	17.316(2)	8.486(4)
α/deg	110.67(2)	—	—	—
β/deg	90.98(3)	103.87(3)	102.42(1)	—
γ/deg	92.92(3)	—	—	—
V/Å^3	1453.3(8)	2656(1)	2719.5(7)	2759(1)
Z	2	4	4	4
μ/cm^{-1}	30.62	22.67	22.28	21.95
$F(000)$/e	572.00	1020.00	1044.00	1024.00
$2\theta_{max}$/deg	137.0	136.5	136.3	120.1
Scan speed/deg min^{-1}	8.0	16.0	16.0	4.0
Scan range/deg	1.73+0.30tan θ	1.78+0.30tan θ	1.68+0.30tan θ	1.00+0.30tan θ
Observed reflections	5485	5290	5439	2385
Reflection used	4045	3248	4121	2359
No. of variables	344	308	317	308
R[a] ($I > 2.00\sigma(I)$)	0.053	0.057	0.059	0.056
R_w[a]	0.053	0.057	0.059	0.058

a) $R = \sum||F_o| - |F_c||/\sum|F_o|$; $R_w = [\sum w(|F_o| - |F_c|)^2/\sum w|F_o|^2]^{1/2}$; $w = 1/\sigma^2(F_o)$.

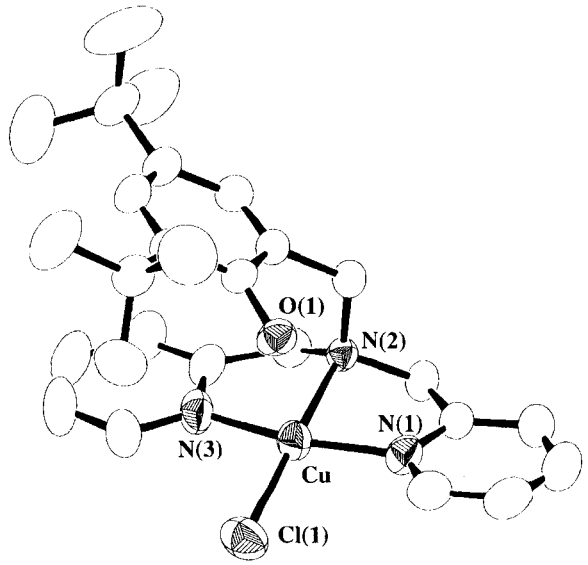

Fig. 3. ORTEP view of the $[CuCl(HtbuL)]^+$ ion in **1** drawn with the thermal ellipsoids at the 50% probability level and atomic labeling scheme.

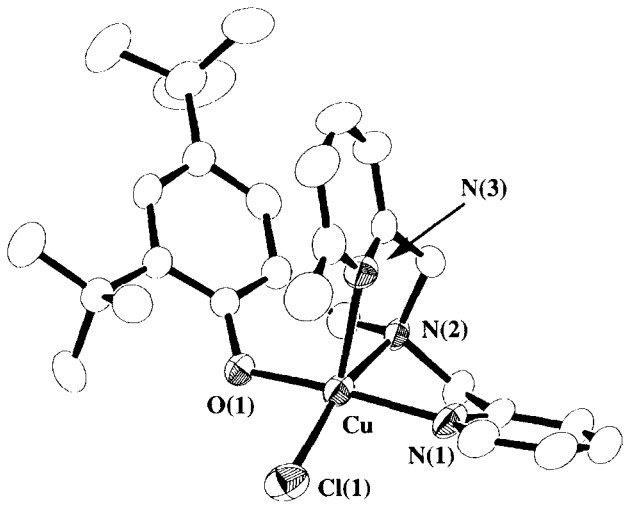

Fig. 4. ORTEP view of the [CuCl(tbuL(Mepy))] (**2**) drawn with the thermal ellipsoids at the 50% probability level and atomic labeling scheme.

center of **1** is calculated to be 0.198 according to the equation $\tau = (\beta - \alpha)/60$, where α = N(1)–Cu(1)–N(2) (164.6°) and β = Cl(1)–Cu(1)–N(3) (176.5°). As τ is zero for a perfect square planar geometry, the structure of **1** may be described as distorted square-planar.

The structure of complex **2** (Fig. 4) differs significantly from that of **1** as it has a deprotonated phenoxide moiety coordinating to the Cu(II) ion with a Cu(1)–O(1) distance of 1.908(3) Å.[20] The Cu(II) coordination plane is formed by one pyridine nitrogen atom, one phenoxide oxygen atom, one tertiary nitrogen atom, and a chloride ion. Probably due to the steric hindrance of the methyl group the 2-methylpyridine moiety is situated in an apical position at a Cu(1)–N(3) distance of 2.329(3) Å, which is longer than that of the apical phenoxide coordinating to Cu in [Cu(bpnp)-

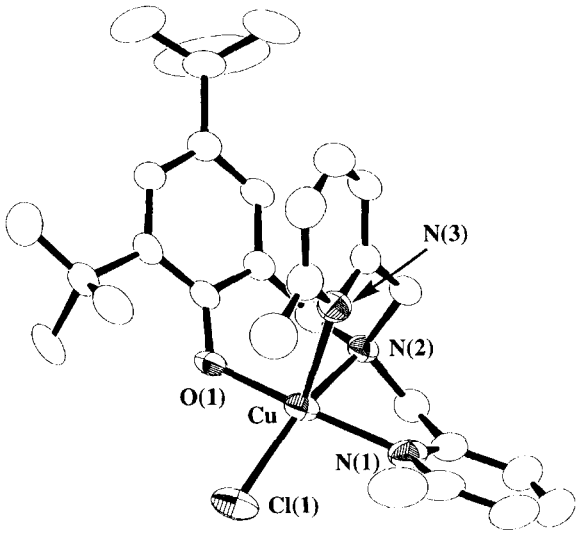

Fig. 5. ORTEP view of $[CuCl(tbuL(Mepy)_2)]$ (**3**) drawn with the thermal ellipsoids at the 50% probability level and atomic labeling scheme.

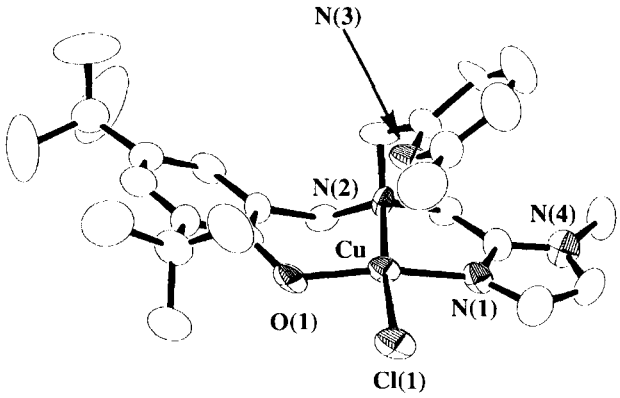

Fig. 6. ORTEP view of [CuCl(tbuL(im)(Mepy))] (**4**) drawn with the thermal ellipsoids at the 50% probability level and atomic labeling scheme.

X][14] but shorter than the Cu(1)–O(1) distance in **1**. The bond lengths between copper and the donor nitrogen atoms Cu(1)-N(1) = 2.025(3) and Cu(1)–N(2) = 2.087(3) Å are virtually the same as those in **1**. The τ value of the Cu center is 0.065 with α = Cl(1)–Cu(1)–N(2) (162.6°) and β = O(1)–Cu(1)–N(1) (166.5°), which suggests that **2** has a nearly perfect square-planar structure. The Cu geometry is described as square-pyramidal with the apical coordination by a pyridine nitrogen.

Complexes **3** and **4** have structures similar to the structure of **2** in the sense that a phenoxide oxygen coordinates to Cu(II) in an equatorial position (Figs. 5 and 6, respectively). The Cu(1)–O(1) distances for **3** and **4** are 1.916(6) and 1.863(9) Å, respectively, the latter of which is the shortest among the complexes obtained. The Cu(II) ion has one pyridine nitrogen, one tertiary nitrogen, one phenoxide oxygen, and one chloride ion in the basal plane, and is in a square-pyramidal geometry with an apical pyridine nitrogen at the Cu(1)–N(3) distance of 2.328(7) Å in **3** which is almost equal to that of **2**. The copper–nitrogen bond lengths in **3** are Cu(1)–N-

Table 2. Selected Bond Distances and Angles

Complex	1	2	3	4
		Bond distance (Å)		
Cu(1)–O(1)	2.559(3)	1.908(3)	1.922(3)	1.863(9)
Cu(1)–N(1)	1.976(3)	2.024(4)	2.099(4)	1.942(9)
Cu(1)–N(2)	2.054(3)	2.097(4)	2.079(3)	2.146(9)
Cu(1)–N(3)	1.982(4)	2.335(4)	2.321(3)	2.538(8)
Cu(1)–Cl(1)	2.240(1)	2.264(2)	2.267(1)	2.303(3)
		Bond angle (deg)		
Cl(1)–Cu(1)–O(1)	94.41(7)	91.5(1)	89.21(8)	92.8(2)
Cl(1)–Cu(1)–N(1)	97.1(1)	93.9(1)	97.6(1)	93.2(3)
Cl(1)–Cu(1)–N(2)	176.46(10)	162.7(1)	156.45(9)	175.0(2)
Cl(1)–Cu(1)–N(3)	96.7(1)	116.3(1)	122.12(10)	103.1(2)
O(1)–Cu(1)–N(1)	90.5(1)	166.5(2)	167.1(1)	160.4(3)
O(1)–Cu(1)–N(2)	87.1(1)	91.5(1)	90.9(1)	91.8(3)
O(1)–Cu(1)–N(3)	93.7(1)	98.7(1)	94.2(1)	106.6(3)
N(1)–Cu(1)–N(2)	82.4(1)	79.8(2)	78.5(1)	81.8(3)
N(1)–Cu(1)–N(3)	165.0(2)	90.0(2)	91.5(1)	90.2(3)
N(2)–Cu(1)–N(3)	83.5(1)	80.0(1)	81.4(1)	77.6(3)

(1) = 2.099(7) and Cu(1)–N(2) = 2.072(7) Å. The Cu–pyridine nitrogen (N(1)) distance is slightly longer than that of complex **2** because of the steric effect of the methyl group of the equatorial pyridine ring.[15] The τ value for the Cu center of **3** is obtained as 0.205 with α = Cl(1)–Cu(1)–N(2) (155.6°) and β = O(1)–Cu(1)–N(1) (160.9°, so that **3** is more distorted from the square-pyramidal structure than **2** owing to the same steric effect. The bond length of Cu–imidazole nitrogen (N(1)) in complex **4**, Cu(1)–N(1) = 1.942(9) Å, is the shortest among the four complexes, reflecting the fact that imidazole is a stronger σ-donor or weaker π-acceptor than pyridine. Considering that the Cu–tertiary nitrogen distance Cu(1)–N(2) = 2.146(9) Å and the Cu–apical nitrogen distance Cu(1)–N(3) = 2.538(8) Å are the longest and that the Cu(1)–O(1) distance (1.863(9) Å) is the shortest among the present complexes, we may infer that the phenoxide oxygen and imidazole nitrogen push their electrons to the Cu(II) ion. The τ value for the Cu center of **4** is 0.250 (α = O(1)–Cu(1)–N(1) (160.1°) and β = Cl(1)–Cu(1)–N(2) (175.0°)), indicating the strongest distortion from the square-planar geometry.

Characterization of the Phenoxide Complexes. Except for **1**, all the Cu(II) complexes are deeply colored due to an absorption peak at λ_{max} = 510—550 nm (ε = 800—1400 M^{-1} cm^{-1}) (Table 3), which we assign to the phenoxide-to-Cu(II) (ligand-to-metal) charge transfer (LMCT).[10b,20] In contrast, complex **1**, where the protonated phenol moiety is situated in an apical position and coordinates only weakly to Cu(II), lacks this band. LMCT occurs only with an equatorially coordinated phenoxide. Comparison of λ_{max} values for the isostructural series **2**, **3**, and **4** shows that the transition energy increases with the decrease of the equatorial Cu–N-(pyridine or imidazole) bond distances in the order 2(6)-methylpyridine (**2**, 543 nm) < unsubstituted pyridine (**3**, 519 nm) < imidazole (**4**, 511 nm).

All of the Cu(II) complexes exhibit axial signals in their X-band ESR spectra (frozen CH_3OH solution at 77 K), which are consistent with a $d_{x^2-y^2}$ ground state ($g_{//} > g_\perp > 2.0$; $|A_{//}|$ = 15—17 mT) (Table 3). Comparison of the $|A_{//}|$ values for **2**, **3**, and **4** shows that they decrease with the increase of the τ values in the order imidazole (**4**, $|A_{//}|$ = 15.0 mT) < unsubstituted pyridine (**3**, $|A_{//}|$ = 15.8 mT) < 2(6)-methylpyridine (**2**, $|A_{//}|$ = 16.9 mT). It is suggested that these compounds in solution maintain the structures revealed in the solid state, since a decrease in the $|A_{//}|$ values reflects, analogous to the increase in the τ values, the distortion from the $d_{x^2-y^2}$ planar state.[10b,19]

One-Electron Oxidation. Addition of one equivalent of $(NH_4)_2[Ce(NO_3)_6]$, a one electron oxidant, to **2**, **3**, and **4** in acetonitrile at low temperature caused a color change from purple to green, and the resulting green solutions were ESR-inactive at 77 K. On the other hand, the ESR spectrum of **1** remained unchanged upon addition of Ce(IV). Oxidized **2**, **3**, and **4** exhibited a new absorption band centered at

Table 3. Absorption and EPR Spectral Data for Cu(II)-Phenoxide Complexes

Complex	LMCT/nm (ε/M^{-1} cm^{-1})	EPR parameter $g_{//}$	$g_\perp$	$\lvert A_{//}\rvert$/mT
[CuCl(HtbuL)]ClO_4 (**1**)	N.D.	2.25	2.07	17.2
[CuCl(tbuLMepy)] (**2**)	519(1400)	2.28	2.07	16.9
[CuCl(tbuL(Mepy)$_2$)] (**3**)	544(800)	2.29	2.07	15.8
[CuCl(tbuL(im)(Mepy)] (**4**)	511(1200)	2.29	2.07	15.0

405—418 nm (ε = 2000—3500), which is characteristic of the phenoxyl radical species coordinated to Cu(II)[9,10,12,13,21] (Table 4). The lack of the ESR signal at 77 K is interpreted as due to the spin–spin coupling between the phenoxyl radical and the Cu(II) ion.[9,10,13] The ESR spectrum of the one-electron oxidized species of [ZnCl(tbuL)] exhibited a radical signal at g = 2.00 and the typical absorption peak at 405 nm (Table 4), demonstrating formation of a radical for the Zn(II) complex on oxidation and thus the Cu(II)–phenoxyl radical state. At 3.5 K, however, the ESR spectra of **2**, **3**, and **4** all showed a low field signal around g = 4.0 due to spin pairs ($S_1 = S_2 = 1/2$) for $\Delta M_s = 2$ transition and a broad signal at $g < 2$ for $\Delta M_s = 1$ (Fig. 7). These results reveal that one-electron oxidized **2**, **3**, and **4** have an S = 1 ground state and that the phenoxyl radical is coordinated to Cu(II).[9b] If the dihedral angle between the Cu(II) coordination plane and the plane of the phenoxyl radical is 0° and the angle Cu(II)–O–C(phenoxyl radical) is 120°, the $d_{x^2-y^2}$ orbital and the SOMO of the radical are orthogonal to each other to make the radical complex ferromagnetic. For the present complexes, the Cu(II)–O–C angles are 118.9—126.7° and the dihedral angles are 23.9—36.5° and closer to 0° than to 90°, so that their radicals may be weakly ferromagnetic. According to the curve fitting using the equation IT = const-$(1+\exp(-J/kT))$, where I, k, and const are the intensity of the ESR signal, Boltzmann's constant, and a constant, respectively,[9b] the constant for the ferromagnetic coupling for **2**, $-2J$ ($H = -2JS_1S_2$), was calculated to be ca. -10 cm^{-1}, which is comparable with the reported value.[9b]

Further evidence for the Cu(II)–phenoxyl radical bonding has been provided by comparison of the resonance Raman spectra between the one-electron oxidized species of **2** and [Zn(tbuL)Cl]. The Raman spectra in the 1100—1700 cm^{-1} range obtained before and after Ce(IV) oxidation of **2** disclosed that the bands observed for **2** disappeared upon oxidation to give an intense band at 1504 cm^{-1}, which corresponded well with the characteristic intense 1509-cm^{-1} band exhibited on one-electron oxidation of [Zn(tbuL)Cl] (Fig. 8). This band is assigned to the C–O stretching mode (ν_{7a}),[22] which is characteristic of the phenoxyl radical species. The

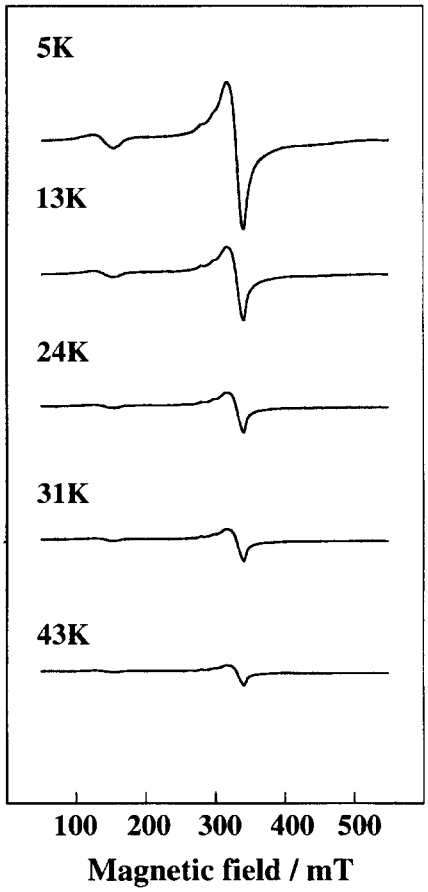

Fig. 7. ESR spectra of one-electron oxidized **2** in CH_3CN.

detected ν_{7a} frequencies of the Cu(II) and Zn(II) complexes were in good agreement with those reported for GO[7] and the Cu(II)- and Zn(II)-coordinated phenoxyl radicals of model compounds,[9a,10,11d] showing formation of a phenoxyl radical.

The strong absorption band at about 400 nm resulting from Ce(IV) oxidation may partly be assigned to a π–π^* transition of the phenoxyl radical.[9–11,12b] The above structure-reactivity relationship suggests that the coordination of the phenoxide is a crucial point, because the apical phenol which coordinates only weakly to Cu(II) dose not give the phenoxyl radical

Table 4. Properties of Phenoxyl Radical Species

Complex	λ_{max}/nm (ε/M^{-1} cm$-$1)	Decay constant/s^{-1} (Half life/min., Temperature/°C)	Redox potential ($E_{1/2}$/V) of Phenoxide/Phenoxyl radical[a)]
[CuCl(HtbuL)]ClO_4 (**1**)	Not determined	Not determined	1.17[b)]
[CuCl(tbuLMepy)] (**2**)	418 (3500) 666 (420)	$(1.86\pm0.04)\times10^{-4}$ (65, −20)	0.56
[CuCl(tbuL(Mepy)$_2$)] (**3**)	406 (2000) 664 (410)	$(1.28\pm0.07)\times10^{-3}$ (9.0, −40)	0.61
[CuCl(tbuL(im)(Mepy)] (**4**)	412 (3000) 659 (420)	$(1.79\pm0.04)\times10^{-4}$ (62, −20)	0.56
[ZnCl(tbuL)] (**5**)	405 (3200) 678 (400)	$(1.31\pm0.05)\times10^{-4}$ (88, −20)	0.69

a) vs. Ag/AgCl. b) Irreversible oxidation peak.

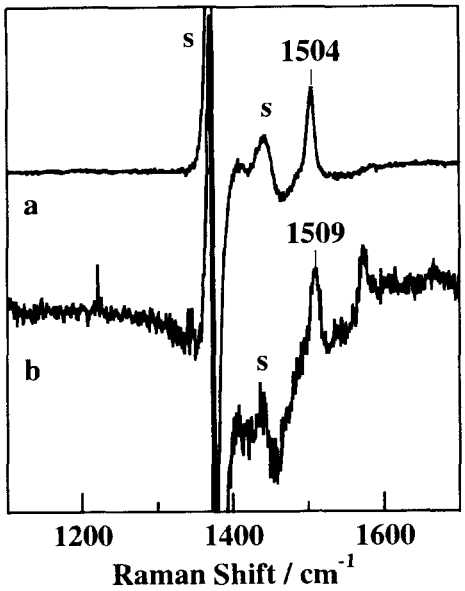

Fig. 8. Resonance Raman spectra of the one-electron-oxidized species of **2** and [ZnCl(tbuL)]; a, **2**; b, [ZnCl(tbuL)]. Solvent peaks are subtracted and s denote the residues from the solvent peaks. The concentration of the sample was 0.5 mM.

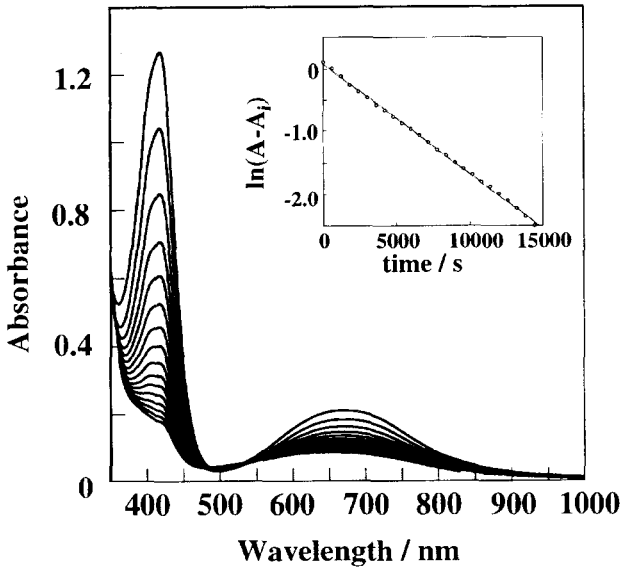

Fig. 9. Absorption spectral change of **2** after one-electron oxidation by 1 equiv of Ce(IV) at −20 °C in CH_3CN (5.0×10^{-4} M). Inset: plot of $\ln[A-A_\infty]$ at 418 nm vs. time.

species. Since the donor ability of the unsubstituted pyridine moiety in **1** is higher than that of the 2(6)-methylpyridine moiety in the other complexes due to the absence of steric hindrance, it may have been difficult for the phenol moiety to coordinate to Cu(II) in the equatorial position in **1**.

The difference between complexes **2**, **3**, and **4** lies in the stability of their phenoxyl radical species. When the green solutions of the oxidized complexes in acetonitrile were left to stand at room temperature under anaerobic conditions, they eventually turned colorless, and accordingly the phenoxyl radical π–π^* transition band at ca. 410 nm disappeared. Plots of the absorbance at the π–π^* band vs. time at −20 °C indicated that the intensity decrease was first-order, as illustrated for **2** in Fig. 9. The decay constants obtained for the radicals of **2**, **3**, and **4** and the half life values calculated from the decay constants are listed in Table 4. The half lives of **2** and **4** were 65 (k_{obs} = $(1.79\pm0.04)\times10^{-4}$ s^{-1}) and 62 min (k_{obs} = $(1.86\pm0.04)\times10^{-4}$ s^{-1}) at −20 °C, respectively, indicating that the stability of phenoxyl radicals is the same for the Cu sites with an unsubstituted pyridine or an imidazole in the equatorial position. In contrast, the half life of **3** was only 9.0 min (k_{obs} = $(1.28\pm0.07)\times10^{-3}$ s^{-1}) at −40 °C, which can be related with the N-donor ability of the equatorial ligand, since **3** has a weaker N donation by the 6-methyl-2-pyridyl group, as viewed from the Cu(1)–N(1) distance of 2.099(7) Å, than that of **2** and **4** for the steric reason described above. A higher energy of the phenoxide-to-Cu(II) LMCT band may indicate a higher stability of the corresponding phenoxyl radical species as seen from the λ_{max} values of 519 and 511 nm for **2** and **4**, respectively, compared with the value of 544 nm for **3**. These results indicate that the stability of the phenoxyl radical species is predominantly influenced by the N-donor ability of the ligand which stabilizes the Cu(II) state.[15]

Cyclic Voltammetry. The cyclic voltammograms of **1**, **2**, **3**, and **4** were recorded in acetonitrile under anaerobic conditions at a scan rate of 50 mV s^{-1} in the range 0—1.0 V where Cu redox waves were not observed except for **1** (Fig. 10). For complex **2**, one quasi-reversible redox wave corresponding to the transfer of one electron was observed at 0.56 V vs. Ag/AgCl (ΔE = 0.11 V) in the same range. Electrolysis at −40 °C of a solution of **2** in CH_3CN (0.1 M TBAP) at 0.85 V showed a transfer of 0.9 electron per mole, and a color change from purple to green was observed. One electron oxidation of **2** yielded an ESR inactive species. The properties of the oxidized species were the same irrespective of electrochemical oxidation and chemical oxidation by Ce(IV). The same redox wave at 0.56 V (ΔE = 0.11 V) was observed for **4**. Complex **3** displayed a similar quasi-reversible redox wave at 0.61 V (ΔE = 0.11 V), i.e. at a slightly higher potential than that for **2** and **4**. On the basis of these results we assign the above oxidation steps to the phenoxide/phenoxyl-radical couple.

On the other hand, complex **1** exhibited a quasi-reversible redox wave with $E_{1/2}$ = 0.03 V (ΔE = 0.11 V) and an oxidation peak at 1.17 V. The first redox step is assigned to the Cu(I/II) redox couple, and the second oxidation peak is suggested to be the oxidation of the phenol moiety. Since the oxidation step is irreversible, **1** does not seem to give a stable one-electron oxidized form owing to the weak coordination structure which is unfavorable for the radical species. Considering that complex **1** could not be oxidized by Ce(IV), we conclude that formation of the phenoxyl radical requires an equatorial coordination of the phenoxide to the Cu center. In this connection, the phenoxyl radical of GO has been assigned to equatorially coordinated Tyr 272, whereas apically

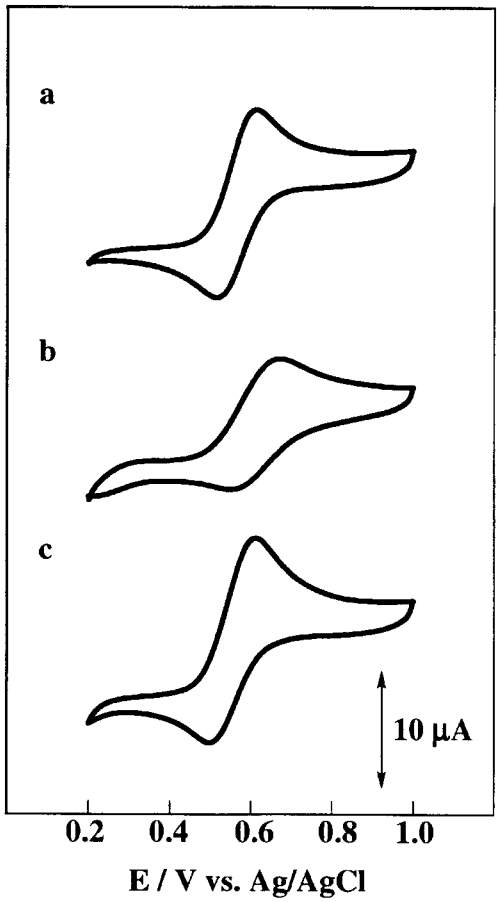

Fig. 10. Cyclic voltammograms of **2**, **3**, and **4** in CH_3CN (1.0×10^{-3} M) containing 0.1 M *n*-Bu_4NClO_4; a, **2**; b, **3**; c, **4**. Working electrode, grassy carbon; counter electrode, Pt wire; reference electrode, Ag/AgCl; scan rate 50 mV s^{-1}.

coordinated Tyr 495 does not form the radical.[1—4]

The properties of the donor groups are an important factor for the stability of the coordinated phenoxyl radical. The higher phenoxide/phenoxyl radical redox potential of complex **3** in comparison to that of **2** or **4** may indicate that the equatorial 2-methylpyridine ring of **3** is a weaker donor than the unsubstituted pyridine and imidazole rings of **2** and **4**, respectively. The phenoxyl radical decay constants (Table 4) show that the radicals of **2** and **4** are more stable than the radical of **3** and that the equatorially coordinated imidazole and unsubstituted pyridine rings are equally effective in stabilizing the radical. In this connection, the redox potential for the phenoxide/phenoxyl radical of GO, $E_{1/2}$ = 0.23 V (vs. Ag/AgCl), is distinctly lower than the values obtained for the present complexes, and the radical species is more stable at room temperature. The difference in the radical stability may be ascribed to two reasons: (1) The apical ligand is a phenol/phenoxide group in GO as compared with the pyridine ring in the present cases. (2) The equatorial phenoxide ring in GO has an *o*-alkylthio group, whereas it has two *t*-butyl groups in our complexes. We reported previously that the Cu(II) complex of a tripodal ligand with an N_2O_2 donor set comprising two phenols and an unsubstituted pyridine has a phenoxyl radical half life of approximately 12 min at −20 °C ($k_{obs} = 9.3\pm0.2\times10^{-4}$),[14] which is much shorter than that for **2** and **4**. This may point to the importance of the *o*-alkylthiophenoxide donor in the stabilization of the active form of GO.

Concluding Remarks. We have prepared and characterized a series of Cu(II) complexes with new tripodal ligands containing one phenol/phenoxide moiety with two *t*-butyl substituents and various pyridine or imidazole rings. At low temperatures, one electron oxidation of the Cu(II) complexes **2**, **3**, and **4** yielded the corresponding Cu(II)–phenoxyl radical species, whose decay constants have been determined. The relationship between the structures of the complexes and decay constants indicates that the Cu(II)–phenoxyl radical species is stabilized by the strong Cu(II)–phenoxide bond; therefore the effective coordination of both the equatorial phenoxide oxygen and pyridine nitrogen donors promotes structural stability. The observed stability of the radical species of **2**, **3**, and **4** may be comparable with that of the tacn-based complexes reported by Tolman et al.,[10] while the Cu complexes by Wieghardt et al. and Stack et al.[9,13] which contain an *o*- or *p*-hetero atom-modified phenoxide moiety are stable at room temperature. The binaphthyl group introduced into the ligand by Stack et al. and probably the sulfur bridge stabilize the Cu(I) state of the complexes, thereby enabling the Cu(I/II) redox cycle. The extra stability of the radical exhibited by GO may be due to the cysteine-modified tyrosine ligand, which is located close to a tryptophan indole moiety. Studies on the effects of hetero atom modification and neighboring aromatic rings on the Cu(II)–phenoxyl binding are in progress in our labolatory.

We are grateful to Dr. Masahiro Sakai, Research Center for Molecular Materials, Institute for Molecular Science, for measurements of ESR spectra at low temperatures. This work was supported in part by a Grant-in-Aid for Scientific Research No. 09304062 from the Ministry of Education, Science, Sports and Culture, for which we express our thanks.

References

1 a) J. W. Whittaker, *Met. Ions Biol. Syst.*, **30**, 315 (1994). b) J. W. Whittaker, in "Bioinorganic Chemistry of Copper," ed by K. D. Karlin and Z. Tyeklár, Chapman & Hall, New York (1993), pp. 447—458.

2 a) N. Itoh, S. E. V. Phillips, C. Stevens, Z. B. Ogel, M. J. McPherson, J. N. Keen, K. D. S. Yadav, and P. F. Knowles, *Nature*, **350**, 87 (1991). b) N. Itoh, S. E. V. Phillips, C. Stevens, Z. B. Ogel, M. J. McPherson, J. N. Keen, K. D. S. Yadav, and P. F. Knowles, *Faraday Discuss.*, **93**, 75 (1992). c) N. Itoh, S. E. V. Phillips, K. D. S. Yadav, and P. F. Knowles, *J. Mol. Biol.*, **238**, 794 (1994).

3 a) M. M. Whittaker, J. W. Whittaker, H. Milburn, and A. Quick, *J. Biol. Chem.*, **265**, 9610 (1990). b) A. J. Baron, C. Stevens, C. Wilmot, K. D. Seneviratne, V. Blakeley, D. M. Dooley, S. E. V. Phillips, P. F. Knowles, and M. J. McPherson, *J. Biol. Chem.*, **269**, 25095 (1994). c) P. F. Knowles, R. D. Brown, III, S. H. Koenig, S. Wang, R. A. Scott, M. A. McGuirl, D. E. Brown, and D. M. Dooley, *Inorg. Chem.*, **34**, 3895 (1995). d) M. P. Reynolds, A. J.

Baron, C. M. Wilmot, E. Vinecombe, C. Steven, S. E. V. Phillips, P. F. Knowles, and M. J. MacPherson, *J. Biol. Inorg. Chem.*, **2**, 327 (1997).

4 J. Stubbe and W. A. van der Donk, *Chem. Rev.*, **98**, 705 (1998).

5 a) G. T. Babcock, M. K. El-Deeb, P. O. Sandusky, M. M. Whittaker, and J. W. Whittaker, *J. Am. Chem. Soc.*, **114**, 3727 (1992). b) G. J. Gerfen, B. F. Bellow, R. G. Griffin, D. J. Singel, C. A. Ekberg, and J. W. Whittaker, *J. Phys. Chem.*, **100**, 16739 (1996).

6 K. Clark, J. E. Penner-Hahn, M. Whittaker, and J. W. Whittaker, *Biochemistry*, **33**, 12553 (1994).

7 M. L. McGlashen, D. D. Eads, T. G. Spiro, and J. W. Whittaker, *J. Phys. Chem.*, **99**, 4918 (1995).

8 G. R. Dyrkacz, R. D. Libby, and G. A. Hamilton, *J. Am. Chem. Soc.*, **98**, 626 (1976).

9 a) A. Sokolowski, H. Leutbecher, T. Weyhermüler, R. Schnepf, E. Bothe, E. Bill, P. Hildebrandt, and K. Wieghardt, *J. Biol. Inorg. Chem.*, **2**, 444 (1997). b) J. Müller, T. Weyhermüler, E. Bill, P. Hildebrandt, L. Ould-Moussa, T. Glaser, and K. Wieghardt, *Angew. Chem., Int. Ed. Engl.*, **37**, 616 (1998). c) P. Chaudhuri, M. Hess, U. Flörke, and K. Wieghardt, *Angew. Chem., Int. Ed. Engl.*, **37**, 2217 (1998). d) P. Chaudhuri, M. Hess, T. Weyhermüller, and K. Wieghardt, *Angew. Chem., Int. Ed. Engl.*, **38**, 1095 (1999). e) P. Chaudhuri, M. Hess, J. Müller, K. Hildebrandt, E. Bill, T. Weyhermüller, and K. Wieghardt, *J. Am. Chem. Soc.*, **119**, 9599 (1999).

10 a) J. A. Halfen, V. G. Young, Jr., and W. B. Tolman, *Angew. Chem., Int. Ed. Engl.*, **35**, 1687 (1996). b) A. Halfen, B. A. Jazdzewski, S. Mahapatra, L. M. Berreau, E. C. Wilkinson, L. Que, Jr., and W. B. Tolman, *J. Am. Chem. Soc.*, **119**, 8217 (1997). c) B. A. Jazdzewski, V. G. Young, Jr., and W. B. Tolman, *Chem. Commun.*, **1998**, 2521.

11 a) J. Hockertz, S. Steenken, S. K. Wieghardt, and P. Hildebrandt, *J. Am. Chem. Soc.*, **115**, 5346 (1993). b) A. Sokolowski, E. Bothe, T. Weyhermüller, and K. Wieghardt, *J. Chem. Soc., Chem. Commun.*, **1996**, 1671. c) B. Adam, E. Bill, E. Bothe, B. Goerdt, G. Haselhorst, K. Hildenbrand, A. Sokolowski, S. Steenken, T. Weyhermüller, and K. Wieghardt, *Chem. Eur. J.*, **3**, 308 (1997). d) A. Sokolowski, J. Müler, T. Weyhermüler, R. Schnepf, P. Hildebrandt, K. Hildebrandt, E. Bothe, and K. Wieghardt, *J. Am. Chem. Soc.*, **119**, 8889 (1997). e) A. Sokolowski, B. Adam, T. Weyhermüller, A. Kikuchi, K. Hildebrandt, R. Schnepf, P. Hildebrandt, E. Bill, and K. Wieghardt, *Inorg. Chem.*, **36**, 3702 (1997).

12 a) M. M. Whittaker, W. R. Duncan, and J. W. Whittaker, *Inorg. Chem.*, **35**, 382 (1996). b) D. Zurita, I. Gautier-Luneau, S. Méage, J.-L. Pierre, and E. Saint-Aman, *J. Biol. Inorg. Chem.*, **2**, 46 (1997). c) S. Itoh, S. Takayama, R. Arakawa, A. Furuta, M. Komatsu, A. Ishida, S. Takamuku, and S. Fukuzumi, *Inorg. Chem.*, **36**, 1407 (1997).

13 a) Y. Wang and T. D. P. Stack, *J. Am. Chem. Soc.*, **118**, 13097 (1996). b) Y. Wang, J. L. DuBois, B. Hedman, K. O. Hodgson, and T. D. P. Stack, *Science*, **279**, 537 (1998).

14 Y. Shimazaki, S. Huth, A. Odani, and O. Yamauchi, submitted for publication.

15 H. Nagao, N. Komeda, M. Mukaia, M. Suzuki, and K.Tanaka, *Inorg. Chem.*, **35**, 6809 (1996).

16 "International Tables for X-Ray Crystallography," ed by J. A. Ibers and W. C. Hamilton, Kynoch, Birmingham (1974), Vol. IV.

17 "Single Crystal Structure Analysis Software," Version 1.8, Molecular Structure Corporation, The Woodlands (1997).

18 a) U. Rajendran, R. Viswanathan, M. Palaniandavar, and M. Lakshminarayanan, *J. Chem. Soc., Dalton Trans.*, **1992**, 3563. b) R. Uma, R. Viswanathan, M. Palaniandavar, and M. Lakshminarayanan, *J. Chem. Soc., Dalton Trans.*, **1994**, 1219. c) M. Vaidyanathan, R. Viswanathan, M. Palaniandavar, T. Balasubramanian, P. Prabhaharan, and T. P. Muthiah, *Inorg. Chem.*, **37**, 6418 (1998).

19 A. W. Addison, T. N. Rao, J. Reedijk, J. von Rijn, and G. C. Verschoor, *J. Chem. Soc., Dalton Trans.*, **1984**, 1349.

20 Cu(II) complexes containing a phenol moiety have been reported: a) K. D. Karlin and B. I. Cohen, *Inorg. Chim. Acta*, **107**, L17 (1985). b) K. D. Karlin, B. I. Cohen, J. C. Hayes, A. Farooq, and J. Zubieta, *Inorg. Chem.*, **26**, 147 (1987). c) H. Adams, N. A. Bailey, D. E. Fenton, Q.-Y. He, M. Ohba, and H. Okawa, *Inorg. Chim. Acta*, **215**, 1 (1994). d) H. Adams, N. A. Bailey, I. K. Campbell, D. E. Fenton, and Q.-Y. He, *J. Chem. Soc., Dalton Trans.*, **1996**, 2233.

21 E. R. Aitwicker, *Chem. Rev.*, **67**, 475 (1967).

22 A. Mukherjee, M. L. McGlashen, and T. G. Spiro, *J. Phys. Chem.*, **99**, 4912 (1995).